Available online at www.sciencedirect.com
ScienceDirect
Journal of Organometallic Chemistry 692 (2007) 2683–2696
Journal of Organometallic Chemistry
www.elsevier.com/locate/jorganchem

# Structures and EPR spectra of binary sulfur–nitrogen radicals from DFT calculations ☆

René T. Boeré [a,*], Heikki M. Tuononen [b], Tristram Chivers [c], Tracey L. Roemmele [a,c]

[a] Department of Chemistry and Biochemistry, The University of Lethbridge, Lethbridge, Alta., Canada T1K 3M4
[b] Department of Chemistry, The University of Jyväskylä, Jyväskylä, FI-40014, Finland
[c] Department of Chemistry, The University of Calgary, Calgary, Alta., Canada T2N IN4

Received 9 October 2006; received in revised form 7 November 2006; accepted 7 November 2006
Available online 23 November 2006

**Abstract**

The scattered electron paramagnetic resonance (EPR) spectroscopic data for binary sulfur–nitrogen (S,N) radicals have been compiled and critically assessed. Many of these are inorganic rings or cages. For each species, possible equilibrium structures in the gas phase and the EPR hyperfine coupling (hfc) constants have been calculated with DFT using the B3LYP functional and basis sets of triple-ζ (or better) quality. Good agreement is obtained between calculated and measured values for the well characterized $[S_3N_2]^{+\bullet}$, a planar π-radical for which the s-component of the orbitals is likely to be reasonably independent of minor geometrical changes between gas-phase and condensed-phase states. The cage compounds $[S_4N_4]^{-\bullet}$ and $[S_4N_5]^{-2\bullet}$, for which reliable experimental EPR spectra have been reported, show larger variation between calculated and measured hfc, as a consequence of the dependence of the s orbital content of the molecular orbitals on small structural changes. The very large disagreements between the DFT calculated and experimentally claimed hfc constants for $[NS]^{\bullet}$, $[SNS]^{\bullet}$ and $[S_4N_4]^{-3\bullet}$ in condensed phases lead us to question their assignment. Among binary S,N radicals, $^{33}S$ hfc data has only been reported for $[S_3N_2]^{+\bullet}$ (through isotopic enrichment). These values were essential for the correct identification of the EPR spectra of this important radical, which previously was misassigned to other species. Our results suggest that $^{33}S$ data will be equally important for the correct identification of the EPR spectra of other binary S,N species, many of which are cyclic systems, e.g. $[S_3N_3]^{\bullet}$, $[S_4N_3]^{\bullet}$ and $[S_4N_5]^{\bullet}$.


*Keywords:* Radicals; Sulfur–nitrogen compounds; EPR spectroscopy; DFT calculations; Hyperfine coupling constants

## 1. Introduction

The literature on free radicals derived from binary sulfur–nitrogen (S,N) compounds remains scattered and incomplete [1]. There have been multiple reports of strong and persistent EPR spectra whose assignments have been revised, or which have never been conclusively identified. For example, after several incorrect assignments, the "five-line" $^{14}N$ spectrum obtained from solutions of both $S_4N_4$ and $S_2N_2$ in concentrated aqueous acid was eventually identified as belonging to the thermodynamically stable $[S_3N_2]^{+\bullet}$ radical by means of $^{33}S$ labeling [2]. Another example is the nine-line pattern obtained on reduction of $S_4N_4$ by elemental potassium in dimethoxyethane [2a], which has not been conclusively identified. The "blue radical" formed upon dissolution of *cyclo*-$S_7NH$ in various

☆ This article is based on an oral presentation by René T. Boeré (Abstract 117) at the 11th International Symposium on Inorganic Ring Systems, Oulu, Finland, July 30–August 4, 2006.

* Corresponding author. Tel.: +1 403 329 2045; fax: +1 403 329 2057.
*E-mail address:* boere@uleth.ca (R.T. Boeré).

0022-328X/$ - see front matter © 2006 Elsevier B.V. All rights reserved.
doi:10.1016/j.jorganchem.2006.11.026

solvents was later shown to be the diamagnetic acyclic anion $[S_4N]^-$ [3]. In addition, reliable assignments have not been made for the EPR spectra of several S,N species reported as recently as 1990 [4].

In 1990 Preston and Sutcliffe reviewed the state of knowledge in EPR spectroscopy of binary S,N radicals. This comprehensive account included a compilation of the known $^{33}S$ hyperfine coupling (hfc) data, mostly derived from their own work, and the extant evidence for other S,N radicals based only on $^{14}N$ data (the majority of cases) [5]. The only binary S,N species for which $^{33}S$ data were available at that time was the $[S_3N_2]^{+\bullet}$ cation radical, which is also the only binary radical for which the full *g* and *a* tensor components have been determined from measurements of anisotropic spectra [5]. An earlier review by Oakley discusses the redox properties of sulfur–nitrogen compounds – including free radicals – in the context of their fundamental chemical and electronic properties [6]. In the intervening 16 years, much additional progress has been made on the EPR characterization of paramagnetic molecular species, particularly neutral C,N,S π-radicals which gain considerable thermodynamic and kinetic stability from the incorporation of carbon in the ring frameworks [7]. For binary S,N species there has been no recent progress on the experimental front, but the published electrochemical data were comprehensively reviewed in 2000 [8].

The emergence of density functional theory (DFT) methods has in the past 10 years revolutionized our ability to calculate the hfc constants for free radicals of the main group elements. Sieiro and co-workers have recently completed a prospective study of 75 radicals containing 14 main group elements, comparing a variety of different functionals and basis sets [9a]. The B3LYP functional was found to be the most reliable, and the use of large triple-ζ basis sets TZVP and EPR-III was recommended for systems up to 10 nuclei. For larger systems, these authors were restricted to the medium-sized 6-31G* basis set (molecules up to 20 atoms were investigated) which still produced reasonable agreement with experimental values [9b]. They report that, using their level of theory, DFT methods provide excellent agreement for $^1H$ hfc constants in many small molecules, but for heavier nuclei the agreement is found to be only sufficiently good to allow the correct assignment of nuclei by their calculated hfc constants in comparison to experimentally determined values. This, they argue, is the most important contribution that theoretical calculations provide for the field of EPR spectroscopy at the current time. More relevant to the present work are the UB3LYP/TZVP results of Gassmann and Fabian from a study of 10 S,N and C,N,S radicals, which demonstrated agreement equivalent to correlated UMP2 ab initio methods compared to available experimental evidence [10]. The DFT method provided an average absolute error of 0.05(1) for $^{14}N$ (13%), 0.12(1) for $^{33}S$ (24%) and 0.04(1) mT for $^1H$ (44%) for these planar π-radicals.

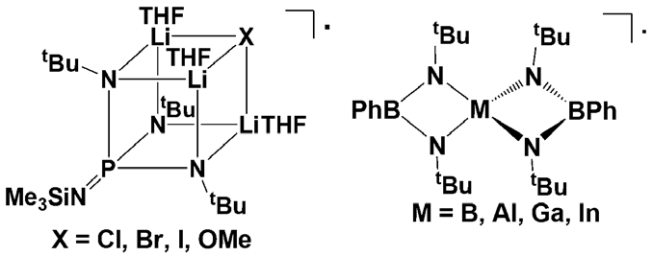


Chart 1. Structures of cubic and spirocyclic main group element radicals [11].

In our own work, we have made use of a variety of DFT methods to assist in the assignment of complex EPR spectra for B, N, Al, P, Ga and In containing radicals (Chart 1) [11]. We found that DFT calculations produce semi-quantitative agreement with the experimental values, and that the calculated values are sufficiently accurate that their input as initial values into extant isotropic EPR simulation software leads to rapid convergence of iterative methods even in the case of very complex experimental spectra [11].

In this paper, we report on DFT calculations of all known and several speculative binary S,N neutral radicals and radical ions containing from two to nine atoms. For systems with more than three atoms we only consider rings or cages. We discuss the structures of these molecules obtained from full geometry optimizations in the gas phase. The geometries are compared with experimental and, where relevant, previous computational evidence, as well as with the known structural data for closely related diamagnetic species. The computed hfc constants are compared with experimental data and the validity of their assignments is evaluated. Finally, we provide a few signposts for the resolution of the many outstanding issues.

## 2. Method

The binary S,N radicals we have considered in this study are listed along with a compilation of reported EPR data in Table 1. For each species, full geometry optimization was conducted using the UB3LYP/(aug)cc-pVTZ level of theory as implemented in GAUSSIAN-98 [12]. The nature of the stationary points found was ascertained by performing frequency calculations and they all correspond to local minima in the potential energy hypersurface. In the case of $[S_4N_3]^{\bullet}$, $[S_4N_4]^{+\bullet}$, $[S_4N_4]^{-3\bullet}$ and $[S_7N]^{\bullet}$ several competing geometries found experimentally for the related diamagnetic species were considered as starting points in the optimizations. The geometries selected for hfc constant calculations correspond to the lowest energy structures found.

The isotropic hfc constants were calculated at the optimized structures using the UB3LYP functional. The

Table 1
DFT calculated and experimental EPR hfc data for binary S,N radicals

| Compound [CAS No.] | Nucleus | Calculated hfc (mT) | Experimental hfc (mT) | Absolute difference (mT) | Percent difference | Reference |
|---|---|---|---|---|---|---|
| $[NS]^{\bullet}$ | $^{14}N$ | 0.65 | 0.765[a] | 0.1 | 15 | [21] |
| [12033-56-6] | $^{33}S$ | 0.19 | – | | | |
| $[SNS]^{\bullet}$ | $^{14}N_1$ | 2.11 | 1.13[b] | 1.0 | 88 | [26] |
| [12033-57-7] | $^{33}S_{1,2}$ | 0.56 | 0.5 | 0.06 | 12 | [4] |
| $[NSN]^{-\bullet}$ | $^{14}N_{1,2}$ | 0.40 | 0.51[c] | 0.1 | 20 | [26] |
| [92614-45-4] | $^{33}S_1$ | 3.08 | 0.45 | 2.63 | 580 | [4] |
| $[S_2N_2]^{+\bullet}$ | $^{14}N_{1,2}$ | 0.78 | [d] | | | |
| [12504-96-0] | $^{33}S_{1,2}$ | −0.29 | – | | | |
| $[S_2N_2]^{-\bullet}$ | $^{14}N_{1,2}$ | 0.63 | – | | | |
| [80182-51-0] | $^{33}S_{1,2}$ | 0.28 | – | | | |
| $[S_3N_2]^{+\bullet}$ | $^{14}N_{1,2}$ | 0.32[e] | 0.31[f] | 0.01 | 3 | [5] |
| [77460-97-0] | $^{33}S_{1,2}$ | 0.78[e] | 0.86[f] | 0.08 | 10 | [5] |
| | $^{33}S_3$ | −0.39[e] | −0.30[f] | 0.09 | 23 | [5] |
| $[S_3N_3]^{\bullet}$ | $^{14}N_{1,2}$ | 0.57 | – | | | |
| [79796-30-8] | $^{14}N_3$ | −0.18 | – | | | |
| | $^{33}S_{1,2}$ | 0.60 | – | | | |
| | $^{33}S_3$ | 0.11 | – | | | |
| $[1,3\text{-}S_4N_2]^{+\bullet}$ | $^{14}N_{1,2}$ | 0.58 | – | | | |
| [88643-34-9] | $^{33}S_1$ | −0.35 | – | | | |
| | $^{33}S_2$ | −0.05 | – | | | |
| | $^{33}S_{3,4}$ | 0.56 | – | | | |
| $[1,3\text{-}S_4N_2]^{-\bullet}$ | $^{14}N_{1,2}$ | 0.63 | – | | | |
| [76858-90-7] | $^{33}S_1$ | 0.71 | – | | | |
| | $^{33}S_2$ | 0.03 | – | | | |
| | $^{33}S_{3,4}$ | −0.07 | – | | | |
| $[S_4N_3]^{\bullet}$ | $^{14}N_{1,2}$ | 0.64 | – | | | |
| [Not assign] | $^{14}N_3$ | −0.33 | – | | | |
| | $^{33}S_{1,2}$ | 0.23 | – | | | |
| | $^{33}S_{3,4}$ | 0.12 | – | | | |
| $[S_4N_4]^{+\bullet}$ | $^{14}N_{1-4}$ | 0.24 | Unresolved[g] | | | [62] |
| [88928-88-5] | $^{33}S_{1,2}$ | 0.92 | – | | | |
| | $^{33}S_{3,4}$ | −0.18 | – | | | |
| $[S_4N_4]^{-\bullet}$ | $^{14}N_{1-4}$ | 0.08 | 0.117[h] | 0.035 | 29 | [64b] |
| [50632-54-7] | $^{33}S_{1,2}$ | −0.65 | – | | | |
| | $^{33}S_{3,4}$ | −0.97 | – | | | |
| $[S_4N_5]^{\bullet}$ | $^{14}N_{1-4}$ | 0.23 | – | | | |
| [Not assign] | $^{14}N_5$ | −0.24 | – | | | |
| | $^{33}S_{1,2}$ | −0.12 | – | | | |
| | $^{33}S_{3,4}$ | 0.49 | – | | | |
| $[S_4N_5]^{-2\bullet}$ | $^{14}N_{1-4}$ | 0.10 | 0.175[i] | 0.075 | 43 | [26] |
| [Not assign] | $^{14}N_5$ | −0.10 | 0.05[i] | 0.05 | 50 | [26] |
| | $^{33}S_{1,2}$ | −0.30 | – | | | |
| | $^{33}S_{3,4}$ | 1.05 | – | | | |
| $[S_7N]^{\bullet}$ | $^{14}N_1$ | 1.90 | 2.6[j] | 0.7 | 27 | [58] |
| [29287-81-8] | $^{33}S_{1,7}$ | 0.27 | – | | | |
| | $^{33}S_{2,6}$ | 0.07 | – | | | |
| | $^{33}S_{3,5}$ | −0.06 | – | | | |
| | $^{33}S_4$ | 0.05 | – | | | |

[a] Fermi-contact term extracted from a gas-phase EPR experiment (see text for explanation); claims for this radical in condensed phases, such as *g*-value = 2.0067(5); $a_N$ = 1.260(5) mT [35] have been questioned [5].
[b] *g*-value = 2.0057; *a* = 1.12 mT [4].
[c] *g*-value = 2.0105(5); *a* = 0.516 mT [35]; *g*-value = 2.013; *a* = 0.55 mT [4]; see also [2a].
[d] The claimed species in [2b] has been identified as $[S_3N_2]^{+\bullet}$.
[e] Previous DFT calculated values: $a_{N1,2} = 0.36$; $a_{S1,2} = 0.56$; $a_{S3} = -0.34$ mT [10].
[f] *g*-value = 2.0115; line-width = 0.08 mT; 22 °C, $D_2SO_4$ [5].
[g] Unresolved singlet, line-width = 4.5 mT, *g*-value = 2.004 [62].
[h] $CH_3CN$, −20 °C; *g*-value = 2.0006(1), *a* = 0.1185 mT, linewidth = 0.05 mT, THF, −25 °C [64a].
[i] Estimated line-width = 0.04 mT, −40 °C; *g*-value not measured [26].
[j] From the trace of the principle components of the hfc tensor in the solid state [58].

basis set used for nitrogen in hfc constant calculations was customized from Partridge's (very large) uncontracted s,p basis set by augmenting it with d and f functions from the cc-pVTZ basis [13]. For sulfur, the plain cc-pVTZ basis set was employed to speed up the calculations.

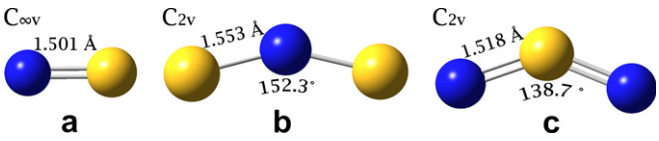


Fig. 1. Geometry-optimized structures of two and three atom binary S,N radicals: (a) [NS]•, (b) [SNS]• and (c) [NSN]•−.

## 3. Results and discussion

The optimized structures, as gas-phase molecules, of the free radicals in this study are depicted in Figs. 1, 5, 7, 9, 11 and 13 and the calculated as well as experimental EPR data, where available, are provided in Table 1. For the larger molecules, atom numbers in the figures match those used in the table. All surface plots present the molecules in the same orientation as the structural diagrams noted above. Full coordinate listings for these structures are provided as Supplementary material.[1]

### 3.1. [NS]•

Far less is known about [NS]• than about the lighter congener, nitric oxide, which plays a significant role in many biological functions [14]. The calculated S–N bond length of [NS]• in the $^2\Pi_{1/2}$ ground state is 1.501 Å (Fig. 1), which may be compared to the experimental value of 1.494 Å from gas-phase spectroscopy [15]. A value of 1.5021 Å was obtained by CCSD(T)/cc-pVQZ calculations [16]. About 40 crystal structures have now been reported in which [NS]• is coordinated via nitrogen to transition metals in a range of different oxidation states [17]. The S–N bond distances in these complexes are reported to range from 1.591 [18] to 1.383 Å [19]. The bond distance in $[NS]^+$ has been established to be 1.440(5) Å by gas-phase photoelectron spectroscopy [20]. The longer bond in the neutral radical is consistent with occupancy of the $\pi^*$ orbital by a single electron, reducing the formal bond order to 2.5 from 3.0 in the cation.

The ground state of [NS]• is diamagnetic because of the opposing spin and orbital angular momentum [5]. The EPR spectrum of the thermally accessible excited $^2\Pi_{3/2}$ state has, however, been detected in the gas phase and the $^{14}$N nuclear hyperfine constant determined to be 2.2 mT [21], a relatively small value that implies small nitrogen s orbital contributions to the total spin density. Unfortunately the gas-phase hyperfine coupling is not directly related to the isotropic hfc observable in the condensed phase (Fermi contact interaction). The Frosch and Foley magnetic hyperfine structure parameters *a–d* (defined in Ref. [22]) have, however, been determined for [NS]• which allows the extraction of the Fermi contact interaction term from the experimental data [23]. This value, calculated to be 0.765 mT, can therefore be directly compared to the results of theoretical calculations [24].

An attempt was made to produce [NS]• by electrolysis of $[NS][SbF_6]$ in a mixture of trifluoroacetic anhydride and trifluoroacetic acid with $[^nBu_4N][BF_4]$ as the electrolyte [25]. In this unusual medium two partly overlapping EPR spectra were obtained even before electrolysis commenced, one of which can probably be assigned to $[S_3N_2]^{+\bullet}$, while the other appears to be an $I = 1$ quintet ($a \sim 0.63$ mT) of $I = 1$ triplets ($a \sim 0.20$ mT), albeit from a spectrum of poor signal-to-noise ratio. A much better spectrum obtained during reactions of various amines with $S_3N_3Cl_3$ at low temperature, which may be related to this second species, has since been published ($a = 0.735$ and 0.175 mT) [4]. Obviously, neither of these spectra are attributable to [NS]. The authors also report that commencement of electrolysis on solutions of $[NS][SbF_6]$ did not appreciably alter the EPR spectra, consistent with the highly irreversible behaviour in voltammetry [25]. Finally, EPR parameters of $a_N = 1.260(5)$ mT with $g = 2.0067(5)$ have been attributed to [NS]• [26]. However, these authors erroneously cite Ref. [27] as the source of these data, the origin of which remains obscure.

It is clear that none of the above experimental data agree very well with our calculated $^{14}$N (0.65) and $^{33}$S (0.19 mT) hfc parameters, nor with the equivalent isotropic $a_N$ value of 0.765 mT extracted from the gas-phase EPR measurements (vide supra), which is, however, in good agreement with our calculation. Moreover, the degeneracy of the SOMO of [NS]• may well prevent the observation of liquid-phase EPR spectra due to exceedingly broad lines in conjunction with rather small hfc constants [5]. This is an important issue, as [NS]• is a leading candidate for involvement in the well-documented re-arrangements of sulfur–nitrogen rings and cages that accompany both redox and nucleophilic reactions [1,6]. If [NS]• is indeed EPR-silent in condensed phases the presence of this key radical may go undetected. In this regard, development of efficient and selective spin traps for this radical would be worth pursuing.

### 3.2. [SNS]•

Our calculations indicate a bent structure for the [SNS]• radical in its $^2A_1$ ground state, with a bond angle of 152° and an S–N bond distance of 1.553 Å (Fig. 1). This is consistent with population of a lone-pair type orbital at N with a single electron, when compared to the linear geometry of the well-characterized $[S{=}N{=}S]^+$ cation, for which the S=N bond lengths are in the range 1.46–1.49 Å [28]. The SOMO is indeed an orbital composed of in-plane sulfur p orbitals and a co-planar anti-symmetric nitrogen sp hybrid (Fig. 2a).

[SNS]• has been detected in the gas phase by mass spectrometry through ion-recombination techniques [29], whereas in condensed phases both the linear asymmetric isomer [NSS]• and the symmetric isomer have been identified from vibrational spectroscopic studies of matrix-isolated species [30]. There have been a number of previous computational studies, and there is good agreement between the best of these calculations and the geometrical

[1] See Appendix A.

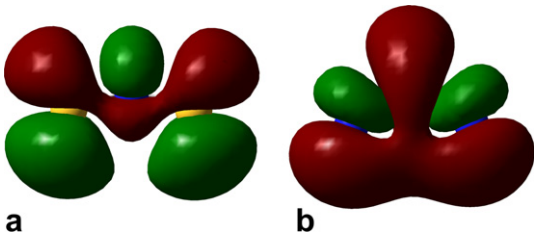


Fig. 2. The Kohn–Sham orbital isosurfaces for the SOMO's of (a) $[SNS]^{\bullet}$ and (b) $[NSN]^{-\bullet}$.

parameters that we report here [31]. For example, Mawhinney and Goddard obtained 1.538 Å for the S–N bond distance from their high-level calculations [31f]; however, to our knowledge, no previous calculations provide hfc constants. Our calculations predict a large coupling to $^{14}N$ and a smaller one to the two $^{33}S$ nuclei (2.11 mT and 0.56 mT, respectively), the latter reflecting the small sulfur atomic s component to the total spin density as a consequence of the almost pure p contribution by S to the SOMO (Fig. 2a).

There are two reports of EPR spectra that may belong to $[SNS]^{\bullet}$ [4,26]. The first is an $I = 1$ triplet with $a_N = 1.13$ mT obtained from a mixture of radicals produced as decomposition products during the room-temperature cathodic reduction of $[S_4N_5]^-$ (at low temperature the dianion radical $[S_4N_5]^{-2}$ is obtained, vide infra) [26]. For comparison: $a_N \sim 5$ mT in the $[ONO]^{\bullet}$ radical [5], and our calculated value for $[SNS]^{\bullet}$ $a_N = 2.11$ mT. The second published spectrum assigned to this radical has $a_N = 1.12$ mT, but with much narrower lines which also allowed for observation of $^{33}S$ coupling of ~0.5 mT at high gain [4]. However, due to the extremely low natural abundance of $^{33}S$, only a very few of the possible satellite lines are visible. It has been noted by several authors that $[SNS]^{\bullet}$ ought to be accessible from chemical or electrochemical reduction of the cation $[SNS]^+$ [5], for which a variety of salts have been prepared [28d,32]. Finally, we note that $^{33}S$ enrichment should lead to very characteristic patterns that would unambiguously identify the elusive $[SNS]^{\bullet}$ radical in the liquid or solid phase by EPR spectroscopy. For example, Fig. 3 shows simulations, using hfc values from our calculations, which predict the appearance of the spectra of this radical at natural abundances of the isotopes and with $^{33}S$ enrichment. While the former is indistinguishable in appearance from the many reported spectra for radicals containing one $^{14}N$ nucleus, the latter has clearly identifiable patterns unique to radicals involving hyperfine coupling to one $^{14}N$ and two $^{33}S$ nuclei.

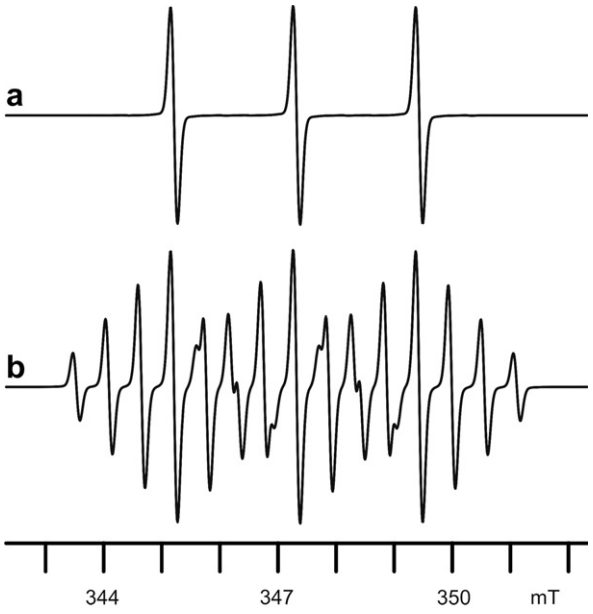


Fig. 3. Simulated EPR spectra for $[SNS]^{\bullet}$ using the calculated isotropic hfc constants (a) with natural abundances of the isotopes and (b) with 99% enrichment in $^{33}S$. Lineshapes have a 30% Gaussian admixture and typical, rather broad, linewidths of 0.12 mT.

### 3.3. $[NSN]^{-\bullet}$

The $[NSN]^{-\bullet}$ radical anion is also calculated to adopt a bent geometry in the gas phase with S–N bond distances of 1.518 Å, and an ∠NSN bond angle of 138.7°. This may be compared to the geometry of $[NSN]^{2-}$, which has only recently been crystallographically characterized, with S–N = 1.484(3) Å and ∠NSN = 129.9(2)° [33]. The increased size of the bond angle in the radical monoanion is consistent with removal of one "lone-pair" like electron from the dianion. The SOMO (Fig. 2b) is indeed an in-plane $a_2$-symmetric orbital dominated by N p and S s atomic orbitals, i.e. an MO that bears a topological resemblance to the SOMO of $[SNS]^{\bullet}$, except that the S and N atoms are transposed. Thus, for $[NSN]^{-\bullet}$ it is the $^{33}S$ nucleus that has the larger calculated hfc constant of 3.08 mT, while the two $^{14}N$ nuclei have quite small calculated hfc constants (0.40 mT) indicative of small s orbital coefficients for N.

The neutral species NSN is a much-speculated reaction intermediate in sulfur–nitrogen chemistry [34]. Many S,N cage compounds show mass spectral fragments resulting from the loss of one S and two N atoms, and moreover display peaks due to the $[N_2S]^+$ ion in electron impact mass spectra [29]. For example, NSN has been proposed as the species eliminated when $R_2PN_5S_3$ cage compounds thermally decompose to $R_2PN_3S_2$ rings [34a]. Surprisingly, the same kind of cage decomposition reactions when either one or both R substituents are F atoms are reported to result in weak EPR signals ($a_N = 0.516(5)$ mT, $g = 2.0105$) attributed to the $[NSN]^{-\bullet}$ radical anion [35]. The red colours mentioned in these reports are, however, not necessarily indicative of the presence of free radicals, as the cyclic products $R_2PN_3S_2$ are intensely red-purple species [34d].

The experimental EPR claims for the $[NSN]^{-\bullet}$ radical are more extensive than for $[SNS]^{\bullet}$. It was first postulated as the species formed when $S_2N_2$ is reduced with metallic potassium in dimethoxyethane [2a]. A very similar spectrum is obtained when $[S_4N_5]^{-\bullet}$ is reduced in $CH_2Cl_2$

solution at room temperature within an EPR electrolysis cell [26]. An analogous EPR spectrum is also obtained when dilute solutions of $[PhCN_3S_2]_2$ are prepared in $CH_2Cl_2$ in air [36]. In all of these measurements, the two equivalent $^{14}N$ nuclei display $a_N \sim 0.50$–$0.52$ mT, in reasonable agreement with our calculated value of 0.40 mT (note that for the heterocycle, assignment to the very similar spectra of dithiadiazolyl free radicals – vide infra – cannot be ruled out). On the other hand, the reported $^{33}S$ hfc for the unique sulfur atom of 0.45 mT is in strong disagreement with the significantly larger calculated value of 3.08 mT [4]. As illustrated in Fig. 4, the identity of this radical could be confirmed by measurement of the EPR spectrum of a $^{33}S$-enriched sample.

The obvious (unambiguous) precursors for the anion radical $[NSN]^{-\cdot}$ are salts of the dianion $[NSN]^{-2}$. Mews has shown that the highly insoluble dipotassium salt, originally reported by Herberhold [37,38], is rendered soluble in organic solvents upon addition of 18-crown-6 [33]. Chivers and Hojo reported that the exhaustive controlled potential electrolysis of $S_4N_4$ at $-2.8$ V vs. $Ag/Ag^+$ produces $[NSN]^{-2}$, and this electrochemical synthesis represents another source of the dianion that may be particularly suitable for producing isotopically enriched samples [39].

### 3.4. $[S_2N_2]^{+\cdot}$

We consider two possible radicals derived from the neutral $S_2N_2$ molecule, a reactive species that is known to polymerize to the superconducting polymer $[SN]_x$ [1]. The calculated structure (Fig. 5) of the cation radical $[S_2N_2]^{+\cdot}$ undergoes considerable distortion from the square-planar structure of the neutral molecule by bending to a $C_{2v}$ geometry with pinching of the NSN and opening of the SNS angles. There is no experimental evidence for the existence

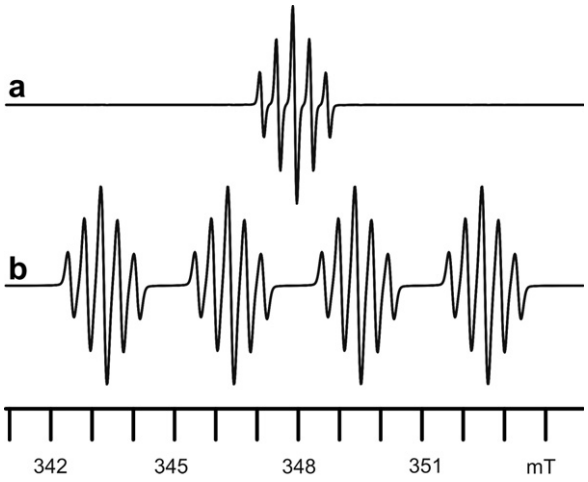


Fig. 4. Simulated EPR spectra for $[NSN]^{-\cdot}$ using the calculated isotropic hfc constants (a) with natural abundances of the isotopes and (b) with 99% enrichment in $^{33}S$. Lineshapes have a 30% Gaussian admixture and typical, rather broad, linewidths of 0.15 mT.

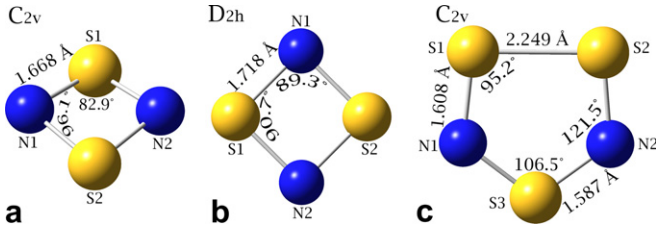


Fig. 5. Geometry-optimized structures of four and five atom binary S,N radicals: (a) $[S_2N_2]^{+\cdot}$, (b) $[S_2N_2]^{-\cdot}$ and (c) $[S_3N_2]^{+\cdot}$.

of this cation (vide infra) and, to our knowledge, there are no previous structure calculations. The crystal structure of $S_2N_2$ is almost square planar with 90.4° and 89.6° bond angles and S–N distances of 1.654 Å [40]. There are also many calculations reported in the literature for neutral $S_2N_2$ [41], which has a complex energy surface [31f]. The marginally longer bonds as well as the folded structure of $[S_2N_2]^{+\cdot}$ are consistent with the loss of an electron from the non-bonding π-symmetric nitrogen-centered orbital in $S_2N_2$ (Fig. 6a).

Early claims in the literature for the formation of the $[S_2N_2]^{+\cdot}$ radical cation from the dissolution of either $S_2N_2$ or $S_4N_4$ in acidic media [2a,2b] have been convincingly re-interpreted in terms of the characteristic $I = 1$ quintet with $a_N = 0.32$ mT of the thermodynamically stable $[S_3N_2]^{+\cdot}$ cation radical [2]. Surprisingly, this assignment resurfaced much later when other workers dissolved $S_2N_2$ in disulfuric acid, but this claim has never been substantiated [42a]. There is therefore no reliable evidence for the existence of $[S_2N_2]^{+\cdot}$ in condensed phases, though Preston and Sutcliffe argue that its detection is to be expected based on a calculated heat of formation of $-1390$ kJ mol$^{-1}$ [5], and it is a common mass spectral fragment [42b]. To our knowledge, no attempts have been made to generate this radical under mild conditions from solutions of the neutral precursor. There is an unpublished report of electrochemical data for $S_2N_2$ in $CH_3CN/[^nBu_4N][BF_4]$ which is mentioned in Ref. [43]; oxidation is reported to occur at +0.1 V and reduction at −0.85 vs. SCE, but no details on the reversibility of either process were provided [8].

### 3.5. $[S_2N_2]^{-\cdot}$

The calculated structure (Fig. 5) of the anion radical $[S_2N_2]^{-\cdot}$ is found to adopt a $D_{2h}$ geometry quite similar to

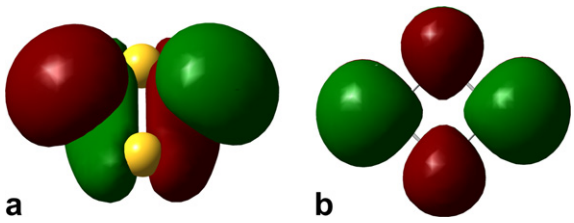


Fig. 6. The Kohn–Sham orbital isosurfaces for the SOMOs of (a) $[S_2N_2]^{+\cdot}$ and (b) $[S_2N_2]^{-\cdot}$.

that of the parent neutral compound. For this species, there is also no experimental evidence for comparison, and only one low-level HF (STO-3G) calculation has been reported [44]. Our calculated bond lengths are longer than that in the neutral molecule by 0.064 Å, and intermediate between that of $S_2N_2$ (1.654 Å) and a typical N–S single bond length (1.74 Å), as might be expected from the population of an anti-bonding π-MO by a single electron (Fig. 6b). It has been suggested that the formation of $[S_2N_2]^{-\bullet}$ in the presence of neutral $S_2N_2$ may induce $\pi^*$-$\pi^*$ coupling between these species, leading to an adduct (i.e. $[S_4N_4]^{-\bullet}$) which could provide a facile pathway for the conversion of $S_2N_2$ to $S_4N_4$ [6]. A similar mechanism was proposed to explain the scrambling of sulfur diimides, RN=S=NR′, which occurs rapidly in presence of a catalytic amount of reducing agent [45]. Whether or not such a mechanism operates, $[S_2N_2]^{-\bullet}$ is likely to be a reactive intermediate, and electrochemical generation at low-temperature concomitant with a careful re-investigation of the voltammetry of $S_2N_2$ solutions probably provides the best hope for its detection in solution. For both $[S_2N_2]^{+\bullet}$ and $[S_2N_2]^{-\bullet}$, $^{33}S$ isotopic enrichment will greatly increase the reliability of an EPR spectral assignment.

### 3.6. $[S_3N_2]^{+\bullet}$

The cation radical $[S_3N_2]^{+\bullet}$, a rigorously planar cyclic π-radical, is by far the best-characterized binary S,N radical. It has been intensively investigated in part because of the false assignment of its EPR spectrum to several other species [2]. Our calculated structure for $[S_3N_2]^{+\bullet}$ is presented in Fig. 5. Several salts in which $[S_3N_2]^{+\bullet}$ exhibits remarkable thermal stability have been structurally characterized by X-ray crystallography [46]. The calculated and experimental structures are in excellent agreement given that the former is in the gas phase and the latter is in the solid state, and that significant lattice interactions between the cation and associated anions are found in the ionic crystals. A full assignment of the hfc and *g* tensors was reported by Preston, Sutcliffe and their co-workers from solid-state experiments in which the radical is doped in a diamagnetic crystal host [47]. It is also worth noting that the isoelectronic replacement of the unique $S^+$ atom in $[S_3N_2]^{+\bullet}$ by an RC group generates a whole family of neutral 1,2,3,5-dithiadiazolyl radicals $[RCN_2S_2]^{\bullet}$, which have been extensively investigated; this family shares the high thermodynamic stability of $[S_3N_2]^{+\bullet}$ [7a,b,e–g,k,8].

The agreement between our calculated and the measured hfc constants is 3% for $^{14}N$ and 10–23% for $^{33}S$. The absolute deviations, which are 0.01 mT for nitrogen, and 0.08–0.09 mT for sulfur, are perhaps more instructive than percentage values. Our calculations provide better agreement between theory and experiment than the results of Gassmann and Fabian (Table 1), but qualitatively the two sets of calculations agree very well [10]. Better agreement between calculated and measured hfc constants is to be expected for rigorously planar π-radicals such as $[S_3N_2]^{+\bullet}$, because minor changes in bond distances and angles are not likely to affect the s character of the total spin density. Conversely, non-planar π radicals such as $[S_4N_4]^{-\bullet}$ (vide infra) or σ-radicals such as $[SNS]^{\bullet}$ or $[NSN]^{-\bullet}$ will have s contributions to the total spin density that are very sensitive to the smallest geometric perturbations. Indeed, for such species the medium itself is likely to influence the structure and hence any measured hfc constants in comparison to calculated gas-phase values. Another consideration, however, is that the magnitude of the coupling constants to both kinds of nuclei in π-radicals such as $[S_3N_2]^{+\bullet}$ is small as a consequence of the low atomic s character of the total spin density. This serves to accentuate the relative uncertainty between calculated and experimental hfc values, even when good agreement is found in absolute terms.

### 3.7. $[S_3N_3]^{\bullet}$

The neutral ring $[S_3N_3]^{\bullet}$ is an elusive member of the binary S,N family [48]. It has been detected by photoelectron spectroscopy in vapors produced from $[SN]_x$ polymer [49], but has never been reliably characterized in condensed phases [50]. The calculated structure (Fig. 7) indicates a planar ring such as is also found in the diamagnetic 10π-electron anion $[S_3N_3]^-$ [51]. Average bond lengths and angles from four simple salts of this anion that are reported in the CCDC database are: S–N = 1.614(20) Å; ∠SNS = 123.6(7)°; ∠NSN = 116.2(4)° [51]. Thus, unlike this precursor, the 9π-electron radical is mildly distorted towards $C_{2v}$ symmetry as a result of a Jahn–Teller effect (Fig. 7a). The best previous calculations reported in the literature for $[S_3N_3]^{\bullet}$ employed only a minimal S,N atomic orbital basis set consisting of (ls6pld/7s3p) contracted to (3s2pld/2slp) and yielded a much more distorted geometry for the radical within the same point-group symmetry: ∠SNS = 138.5, 129.2°; ∠NSN = 109.2, 109.8°; S–N = 1.667, 1.707, 1.740 Å [49].

Although the geometrical distortions in $[S_3N_3]^{\bullet}$ are quite small, the effects these changes have on the calculated hfc constants are very significant, with a factor of three difference in the two kinds of $^{14}N$ coupling, and five for $^{33}S$. Fritz and Bruchhaus attempted to generate $[S_3N_3]^{\bullet}$ by the electrolytic oxidation of $[PPN][S_3N_3]$ in $CH_2Cl_2$ solution containing $[^nBu_4N][BF_4]$ electrolyte [25]. Despite an apparently reversible CV response for the oxidation process, these authors were unable to detect any radicals by EPR

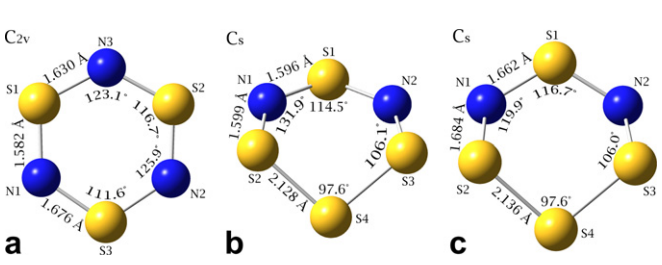


Fig. 7. Geometry-optimized structures of six atom binary S,N radicals: (a) $[S_3N_3]^{\bullet}$, (b) $[1,3\text{-}S_4N_2]^{+\bullet}$ and (c) $[1,3\text{-}S_4N_2]^{-\bullet}$.

spectroscopy upon in situ electrolysis. However, these experiments appear to have been conducted at room temperature, and the lifetime of the neutral radical may simply be too short for observation under their conditions.

### 3.8. $[1,3\text{-}S_4N_2]^{+\cdot}$ and $[1,3\text{-}S_4N_2]^{-\cdot}$

The calculated structures of these radicals are presented in Fig. 7. Whereas the former shows a planar S–N=S=N–S fragment, the latter has a lower bond order, and consequently puckers into a chair conformation. The calculated structures may be compared with the crystal structure of the neutral precursor, 1,3-$S_4N_2$, which like $[1,3\text{-}S_4N_2]^{+\cdot}$ has an envelope conformation with the central S atom of the $S_3$ unit tipped out of the plane of the remaining nuclei [52]. The crystallographic bond distances in 1,3-$S_4N_2$ (numbering as in Fig. 7) are: $S_1$–$N_1$, 1.561(4), $N_1$–$S_3$, 1.676(4), $S_3$–$S_2$, 2.061(2) Å, while the bond angles are: $\angle N_1S_1N_2$, 122.9(2), $\angle S_4N_1S_3$, 126.7(2), $\angle N_1S_3S_2$, 103.4(2) and $\angle S_3S_2S_4$, 102.92(9)°. Thus, the N=S=N and S–S bonds are longer in $[1,3\text{-}S_4N_2]^{+\cdot}$, but the adjacent S–N bonds are shorter; the NSN angle decreases significantly, while the SNS angle opens up somewhat. These changes are consistent with single occupancy of the 7a″ HOMO of neutral 1,3-$S_4N_2$, which is "π-like", non-bonding in N=S=N and anti-bonding in the adjacent S–N region (see the SOMO plot in Fig. 8b) [52].

Preston and Sutcliffe used gas-phase calculated heats of formation to predict a high likelihood for observation of $[S_4N_2]^{+\cdot}$ [5]. This radical is predicted to have its spin density delocalized over the planar S–N–S–N–S substructure, with the highest density on the two "terminal" S atoms (Fig. 8b). An EPR spectrum from a $^{33}$S-enriched sample will be dominated by two equivalent nitrogen and two equivalent sulfur hfc's, and, thus, should be easily recognizable. To our knowledge, no investigation of the electrochemical oxidation of $S_4N_2$ has ever been undertaken.

The structural changes between the neutral precursor and $[1,3\text{-}S_4N_2]^{-\cdot}$ are consistent with occupation of the N=S=N antibonding LUMO of $[1,3\text{-}S_4N_2]$. The bond angles in the anion are all much closer to the ideal tetrahedral angles, compared to those of either the neutral compound or the radical cation (vide supra). The spin density in the $[1,3\text{-}S_4N_2]^{-\cdot}$ radical anion is concentrated on the N–S–N region of the molecule, resulting in significant hfc to two nitrogen and one sulfur nucleus (the SOMO is presented in Fig. 8c.) The EPR spectrum of this species would also be more easily identified with $^{33}$S labeling, because the $S_1$ hfc constant is predicted to be considerably smaller than that in $[NSN]^{-\cdot}$. Chivers and Hojo studied the reduction of neutral $S_4N_2$ by polarography and rotating-disk-electrode voltammetry [53] and concluded that "the initial reduction product of 1,3-$S_4N_2$, presumably the radical anion $[1,3\text{-}S_4N_2]^{-\cdot}$, is unstable with respect to disproportionation to other binary sulfur–nitrogen anions". Thus it appears that this will be a challenging species to observe by EPR spectroscopy.

### 3.9. $[3,5,7\text{-}S_4N_3]^{\cdot}$

The calculated structure of this neutral seven-atom ring is shown in Fig. 9. It consists of an essentially planar N–S–N–S–N fragment, joined by a puckered –S–S– unit that imparts chirality to the structure. The geometry of the $[S_4N_3]^{\cdot}$ radical has not previously been investigated, but recent B3LYP/6-311+G** calculations on the cation indicate a totally planar structure with shorter $S_1$–$N_3$ (1.572 Å) and $S_1$–$N_1$ (1.566 Å) bonds [54]. An early crystallographic study of $[S_4N_3][NO_3]$ also showed a planar structure, and yielded average values of 1.522 and 1.557 Å for these same two sets of bonds [55]. The increases in these bond lengths in the calculated structure of $[S_4N_3]^{\cdot}$ are in accord with population of the $\pi^*$ SOMO in the neutral radical by a single electron (Fig. 10a).

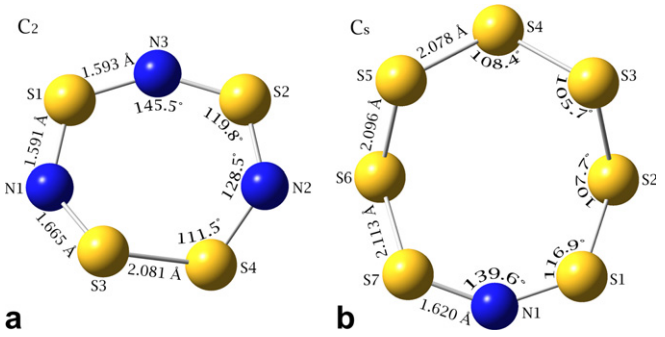


Fig. 9. Geometry-optimized structures of seven and eight atom binary S,N radicals: (a) $[S_4N_3]^{\cdot}$ and (b) $[S_7N]^{\cdot}$.

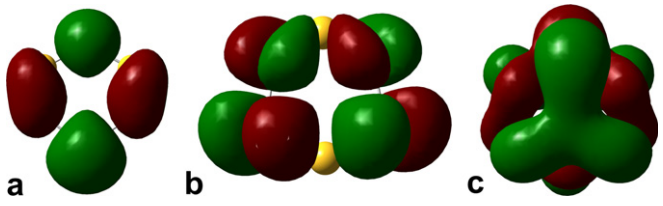


Fig. 8. The Kohn–Sham orbital isosurfaces for the SOMOs of (a) $[S_3N_3]^{\cdot}$, (b) $[1,3\text{-}S_4N_2]^{+\cdot}$ and (c) $[1,3\text{-}S_4N_2]^{-\cdot}$.

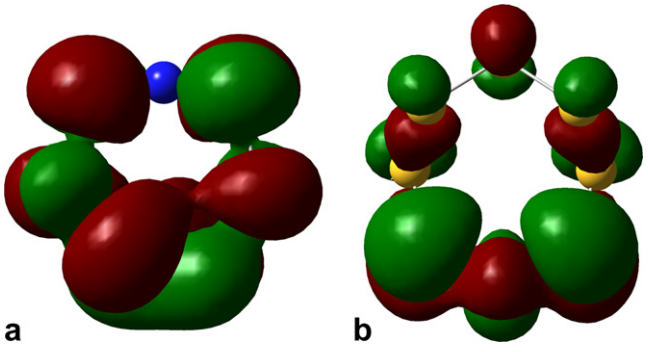


Fig. 10. The Kohn–Sham orbital isosurfaces for the SOMOs of (a) $[S_4N_3]^{\cdot}$ and (b) $[S_7N]^{\cdot}$.

The spin density calculated for $[S_4N_3]^{\bullet}$ is very evenly distributed over the whole ring including the puckered –S–S– section (except for $N_3$, which is nodal in the SOMO, see Fig. 10a), and this delocalization may afford stability to the radical. The calculated hfc constant for the outer two N nuclei is twice as large (0.66 mT) as that of the central N (−0.33 mT), for which hfc is a result of spin polarization. The small calculated values for the $^{33}S$ hfc (0.12 and 0.23 mT) belie rather large spin densities, even for the non-planar –S–S– fragment; the sulfur contributions to the SOMO must be largely confined to p type functions, as is also apparent from Fig. 10a. The $[S_4N_3]^{\bullet}$ radical can likely be generated by one-electron reduction of the corresponding cation. We are not aware of any published electrochemical studies on this classic cationic S,N ring system likely due to the insolubility of salts such as $[S_4N_3]Cl$ [56]. We note, however, that isotopically enriched $[S_4{}^{15}N_3]Cl$ may be prepared from $[^{15}NH_4]Cl$ [57].

### 3.10. $[S_7N]^{\bullet}$

The calculated structure of $[S_7N]^{\bullet}$ predicts a bond angle of 139.6° at nitrogen (Fig. 9). This value is smaller than the 152.3° obtained for neutral $[SNS]^{\bullet}$, suggesting that the smaller angle in the cyclic system may be caused by ring strain from the "bridging" $S_5$ chain. An analysis of the SOMO (Fig. 10b) reveals that, unlike $[SNS]^{\bullet}$ in which in-plane orbitals are involved, the unpaired spin density is concentrated in p orbitals that are perpendicular to the SNS plane. Indeed, in $[S_7N]^{\bullet}$ the in-plane orbitals that correspond to the SOMO of $[SNS]^{\bullet}$ are involved in bonding of the SNS unit to the $S_5$ fragment in the cyclic radical. All the calculated hfc constants for $[S_7N]^{\bullet}$ are smaller than those in $[SNS]^{\bullet}$, but in approximately similar ratios.

An EPR spectrum purported to belong to this radical has been reported from γ-irradiation of $S_7NH$ powders and crystals [58]. The trace of the hfc tensor measured from these solids gives an estimated isotropic coupling of ~2.6 mT, in reasonable agreement with our calculated value of 1.90 mT. A logical precursor for the generation of $[S_7N]^{\bullet}$ is the corresponding anion $[S_7N]^{-}$ which has been characterized by $^{14}N$ and $^{15}N$ NMR spectroscopy in liquid ammonia [59]. However, the thermal instability of this anion will make chemical or electrochemical generation of the radical a very challenging proposition.

### 3.11. $[S_4N_4]^{+\bullet}$

We next consider three radicals derived from the most important binary S,N compound, the neutral cage compound $S_4N_4$. Despite being known since 1835 [1], interest in this compound remains active. The calculated ground-state structure for the 11 π-electron system $[S_4N_4]^{+\bullet}$ is shown in Fig. 11. It is a planar species like the corresponding dication $[S_4N_4]^{2+}$ [60], but the monocation radical has $D_{2h}$ symmetry due to Jahn–Teller distortion. The $S_3$–$N_1$ (and symmetry related) set of bonds are shorter than the

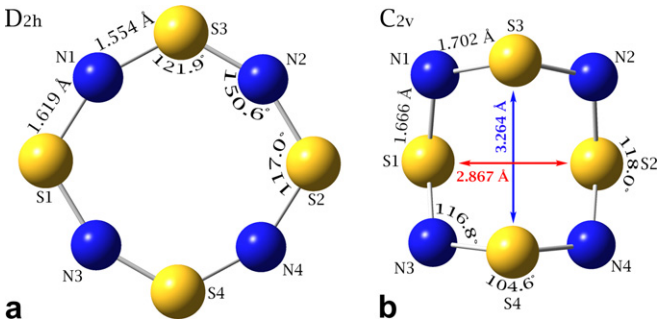


Fig. 11. Geometry-optimized structures of eight atom binary S,N radicals derived from $S_4N_4$: (a) $[S_4N_4]^{+\bullet}$ and (b) $[S_4N_4]^{-\bullet}$.

$S_1$–$N_1$ set, and approach those of an N=S=N unit. In three different salts of $[S_4N_4]^{2+}$, crystallographic studies provide average (with std. dev.) N–S bond distances of 1.550(7) Å and angles: ∠NSN = 118.5(7)°, ∠SNS = 151(2)° [60]. Although a comparison of X-ray and computed bond lengths is not straightforward, the changes in the radical cation geometry seem to be fully consistent with population of the π* SOMO (Fig. 12a), which is antibonding for $S_1$–$N_1$, but essentially non-bonding for $S_3$–$N_1$. The salt $[S_4N_4][FeCl_4]$ has been claimed [61a], but the structural parameters of the cation indicate it is the protonated species $[S_4N_4H]^{+}$ [61b].

The geometry of $[S_4N_4]^{+\bullet}$ is reminiscent of that found in planar, 10 π-electron 1,5,2,4,6,8-dithiatetrazocine rings ($R_2C_2N_4S_2$) [62], which have average N–S–N bond distances of 1.565 Å and mean angles at sulfur of 127.0° [62]. By this analogy, the $S_{1,2}$ atoms in $[S_4N_4]^{+\bullet}$ will have $S^{+}$ character, consistent with the longer N–S bond distances and the smaller bond angle; the calculated Mulliken charges validate this conclusion.

The reported EPR spectrum of $[S_4N_4]^{+\bullet}$ is a ~4.5 mT broad, featureless, signal generated in frozen $CFCl_3$ solutions using γ-irradiation [63]. The average $g$ value of this spectrum is 2.004, and the lack of resolved $^{14}N$ hfc was interpreted by the authors to indicate it to be a π*-radical (SOMO depicted in Fig. 12a), i.e. to have a planar structure, with small hfc to the four equivalent nitrogen nuclei. We question the correctness of this assertion as $[S_3N_2]^{+\bullet}$ is

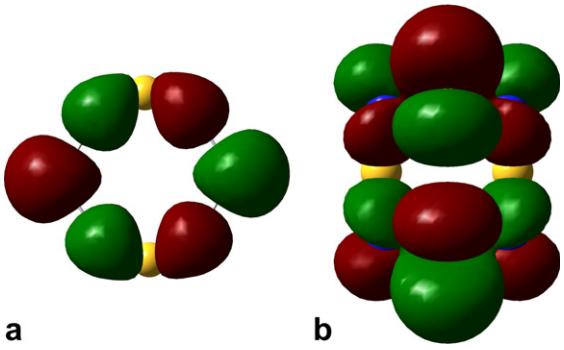


Fig. 12. The Kohn–Sham orbital isosurfaces for the SOMOs of (a) $[S_4N_4]^{+\bullet}$ and (b) $[S_4N_4]^{-\bullet}$.

also a planar $\pi^*$-radical, but has beautifully resolved and easily detectable (>0.5 mT) $^{14}N$ hfc (vide supra). In addition, our calculated hfc values for $[S_4N_4]^{+\cdot}$ are 0.32 mT ($a_N$) and 0.78 and −0.39 mT ($a_S$) and are, therefore, not unlike those found for $[S_3N_2]^{+\cdot}$.

There are no reports of the generation of the $[S_4N_4]^{+\cdot}$ radical cation in a host lattice, for example in salts of $[S_4N_4]^{2+}$, which proved to be very successful in a comprehensive study of $[S_3N_2]^{+\cdot}$ [2], providing the opportunity to measure the full *a* and *g* tensors. A similar study conducted for $[S_4N_4]^{+\cdot}$ would be able to substantiate, or contradict, the report of its identification in the matrix [63]. Attempts to generate the radical cation from chemical oxidation in solution phase have also been tried and have failed [2a]. Similarly, there is no evidence in the literature for an electrochemical oxidation process for $S_4N_4$ at accessible potentials [8]. This is consistent with Oakley's assessment that binary S,N compounds are difficult to oxidize, and that the synthesis of salts of $[S_4N_4]^{2+}$ requires very strong oxidizing conditions such as $AsF_5/SO_2$ or $(FSO_3)_2/HSOF_3$ [6].

### 3.12. $[S_4N_4]^{-\cdot}$ and $[S_4N_4]^{-3\cdot}$

The anion radical $[S_4N_4]^{-\cdot}$ is the next-best characterized S,N free radical after $[S_3N_2]^{+\cdot}$, but there all resemblance ends. Whereas the latter is a thermodynamically stable planar π-radical, $[S_4N_4]^{-\cdot}$ is a reactive, short-lived intermediate (half-life = 27 s at −20 °C) that has only been identified through in situ electrolysis at low temperatures [64]. It seems unlikely that salts of this unstable radical anion will ever be isolated to allow for experimental determination of its structure.

To our knowledge, there is only one previous report of a theoretical study of $[S_4N_4]^{-\cdot}$ which was done at an inadequate HF level (STO-3G) and is omitted from further discussion [44]. Our calculated structure is shown in Fig. 11, in which the expected Jahn–Teller distortion of the $D_{2d}$ structure of the neutral $S_4N_4$ cage leads to a symmetry-lowered $C_{2v}$ geometry in which all four nitrogen atoms remain equivalent (consistent with the known EPR evidence, vide infra) [64a]. The structure of neutral $S_4N_4$ has been determined by gas-phase electron diffraction to have the same $D_{2d}$ symmetry known from X-ray diffraction studies [65]. In the following list, the gas-phase diffraction values are presented in normal text, and that from the recent X-ray structure re-determination are in italics [65]: the S–N distance is 1.623(4), *1.629(1)* Å, the transannular S···S distance is 2.666(14), *2.598* Å, ∠NSN = 105.3(7)°, *104.5(1)*° and ∠SNS = 114.2(6)°, *112.7(1)*°. Thus, in the anion, all the bond lengths are increased, and all the bond angles are opened up, as expected from population of the weakly π(SN) anti-bonding character of the LUMO of the parent species $S_4N_4$. Moreover, one of the two transannular S···S contacts of the $D_{2d}$ neutral cage has opened up much more than the other, as a consequence of the strongly S···S anti bonding character of the LUMO (Fig. 12b). The structure that we obtain is doubly degenerate, and consistent with this, the lowest calculated vibrational frequency for $[S_4N_4]^{-\cdot}$ is a mode that interconverts the long and short transannular contacts.

The monoanion radical $[S_4N_4]^{-\cdot}$ was originally assigned to Chapman and Massey's "nine-line" pattern from chemical reduction of $S_4N_4$ with alkali metal (vide supra) [2a] but, subsequently, $[S_4N_4]^{-\cdot}$ was reassigned to the spectrum obtained by low-temperature in situ electrolysis from $S_4N_4$ inside an EPR resonant cavity [64]. The new nine-line pattern also indicates four equivalent $^{14}N$ nuclei, with $a_N$ reported as 0.1185 mT in THF at −25 °C [64a] or 0.117(20) mT in $CH_3CN$ at −20 °C [64b]. The linewidth at −25 °C in THF was reported to be 0.046 mT, but was found to broaden to ~0.08 mT in the presence of excess $[S_4N_4]$; an effect attributed to rapid electron exchange between the radical and the parent species [64a]. The experimental $a_N$ values are in reasonable agreement with our calculated value of 0.08 mT, and fit much better than the 0.322(4) mT of the Chapman and Massey spectrum [2a]. Since the flexible nature of this radical anion (as shown by our frequency calculation) implies that vibrational averaging will affect the agreement between solution-phase experiment and gas-phase calculation, it is unlikely that better agreement can be expected for this kind of radical. We are therefore very confident that the Myers/Prater spectrum is correctly attributed to $[S_4N_4]^{-\cdot}$. We note also that the calculated geometry has two inequivalent pairs of S nuclei, which are predicted to have quite distinct $^{33}S$ hfc constants. Hence $^{33}S$ substitution may be able to substantiate the predicted structure, so long as the above-mentioned vibrational motion connected to the interchange of the two degenerate conformations is slow on the EPR timescale.

Finally, we briefly consider the origin of the well-resolved nine-line spectrum of an indefinitely stable radical with $a(^{14}N) = 0.322(4)$ mT and LW of ~0.03 mT discovered by Chapman and Massey [2a] and also observed by Jolly and co-workers [2c]. The former authors tentatively attributed this EPR spectrum to the trianion radical $[S_4N_4]^{-3\cdot}$ [2a]. The original study involved potassium metal reduction of $S_4N_4$ in dimethoxyethane [2a]. Jolly and co-workers employed the milder reducing agent sodium naphthalide in THF, which produced several different S,N radicals; the nine-line pattern was only obtained after long reaction times [2c]. Thus it appears that this nine-line pattern is not derived from a radical directly related to reduction of $[S_4N_4]$. We have examined the complex energy surface of $[S_4N_4]^{-3\cdot}$ with DFT calculations and found several local minima; none of these have four symmetry equivalent nitrogen atoms.

### 3.13. $[S_4N_5]^{\cdot}$

The structure of this neutral radical in the gas phase is shown in Fig. 13a. It consists of a bicyclic cage structure that is reminiscent of both related diamagnetic species,

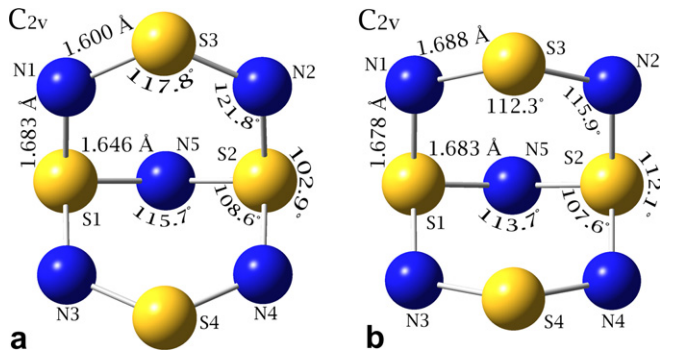


Fig. 13. Geometry-optimized structures of the nine atom binary S,N radicals derived from $[S_4N_5]^+$ or $[S_4N_5]^-$: (a) $[S_4N_5]^\bullet$ and (b) $[S_4N_5]^{2-\bullet}$.

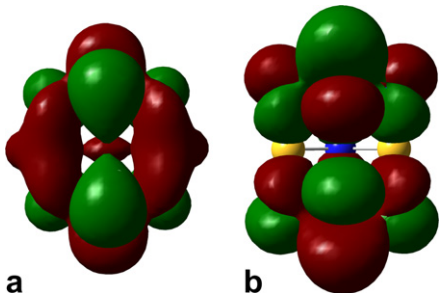


Fig. 14. The Kohn–Sham orbital isosurfaces for the SOMOs of (a) $[S_4N_5]^\bullet$ and (b) $[S_4N_5]^{-2\bullet}$.

$[S_4N_5]^+$ and $[S_4N_5]^-$ [1]. The structure displays two essentially planar S–N–S–N–S fragments that share their "terminal" $S_{1,2}$ atoms (which atoms are also bridged by the unique $N_5$ atom.) The crystal structures of several salts of the diamagnetic cation, namely $[S_4N_5]X$ ($X = Cl^-$, $1/2[Ti_2Cl_{10}]^{-2}$, $[AsF_6]^-$), have been reported [66]. Curiously, a covalent modification, $[S_3N_5SCl]$, has recently been discovered; the structure is analogous to that found for $[S_3N_5SF]$ [67]. For comparison purposes, we refer to the published B3LYP/6-311+G* calculation, in which $S_3$–$N_1$ is 1.575, $S_1$–$N_1$ 1.727 and $S_1$–$N_5$ 1.646 Å [67a].

Only one low-accuracy X-ray diffraction study of the other diamagnetic parent species $[S_4N_5]^-$ is known: $[^nBu_4N][S_4N_5]$ [68]. The average $S_3$–$N_1$ distance is 1.61(2), $S_1$–$N_1$ 1.66(2) and $S_3$–$N_5$ 1.66(2) Å, and the transannular S···S distance is 2.71(2) Å [68]. The geometrical parameters are collected together in Table 2 for easy comparison. Despite the difficulties inherent in comparing X-ray crystallographic and DFT calculated geometrical parameters, it seems clear that the calculated structure for the neutral radical is intermediate for most parameters between those of the corresponding cation and anion. The small predicted changes are consistent with population of the LUMO of $[S_4N_5]^+$, a π-anti-bonding orbital over the N=S=N portions of the molecule (see the SOMO plot in Fig. 14a).

To our knowledge, the observation of this neutral S,N radical has not been reported. Fritz and Bruchhaus observed no radical species when $[^nBu_4N][S_4N_5]$ was subjected to oxidative electrolysis inside an EPR cavity [26], and the CV for the oxidation process was found to be irreversible under all conditions that they investigated.

Table 2
Average bond distances (Å) in $[S_4N_5]^x$ cages

| | $S_3$–$N_1$ | $S_1$–$N_1$ | $S_1$–$N_5$ | S···S | Source |
|---|---|---|---|---|---|
| $[S_4N_5]^+$ | 1.549 | 1.686 | 1.607 | | X-ray, $AsF_6^-$ [66b] |
| $[S_4N_5]^+$ | 1.552 | 1.681 | 1.629 | 4.01 | X-ray, $Cl^-$ [66a,67a] |
| $[S_4N_5]^+$ | 1.575 | 1.727 | 1.609 | | B3LYP/6-311+G* [67a] |
| $[S_4N_5]^\bullet$ | 1.600 | 1.683 | 1.646 | 3.836 | This work |
| $[S_4N_5]^-$ | 1.60 | 1.64 | 1.66 | 2.71 | X-ray, $TBA^+$ [68] |
| $[S_4N_5]^{-2\bullet}$ | 1.688 | 1.678 | 1.683 | 3.341 | This work |

### 3.14. $[S_4N_5]^{-2\bullet}$

The calculated structure of the radical dianion $[S_4N_5]^{-2\bullet}$ in the gas phase is shown in Fig. 13b. Compared to the crystal structure of $[^nBu_4N][S_4N_5]$ (Table 2) [68], we observe a general lengthening of each bond in the dianion, which is consistent with population of the SOMO of $[S_4N_5]^-$, a π-anti-bonding orbital over the N=S=N portions of the molecule (Fig. 14b). This orbital is also anti-bonding with respect to the transannular S···S interaction, which explains the large increase in this parameter in the dianion (a change accomplished by bending the two N=S=N portions of the molecule apart). Note that, unlike $[S_4N_5]^\bullet$ and $[S_4N_5]^+$, but similar to $[S_4N_5]^-$, the S–N–S–N–S fragment does not remain planar in $[S_4N_5]^{-2\bullet}$.

The electronic structure of $[S_4N_5]^{-2\bullet}$ is reminiscent of the calculated structure for $[S_4N_4]^{-\bullet}$ (vide supra). As a consequence, the computed hfc to the N and S nuclei that correspond to those in $[S_4N_4]^{-\bullet}$ are also very similar, and the coupling to the unique nitrogen nucleus is very small. The experimental EPR spectrum of $[S_4N_5]^{-2\bullet}$ was obtained by Fritz and Bruchhaus by electrochemical reduction of $[^nBu_4N][S_4N_5]$ in $CH_2Cl_2$ solution at −40 °C (at higher temperatures, only signals from decomposition products were obtained, vide supra) [26]. The EPR data show the expected large nonet for coupling to the four equivalent $^{14}N$ nuclei of the cage ($a_N = 0.175$ mT), each line of which is further split into a partly resolved triplet from the smaller hfc to the unique $^{14}N$ nucleus ($a_N = 0.05$ mT). This latter coupling is only slightly larger than the experimental linewidth of 0.04 mT. The lifetime of this radical was not investigated and neither has a *g* factor been reported [26].

Compared to the experimental values, we see relative disagreement of 75% and 50% for the bigger and smaller $^{14}N$ hfc constants and the absolute agreement is 0.08 and 0.05 mT, respectively. Here too, the large relative errors reflect the small absolute values of the coupling constants. There is no report of $^{33}S$ hfc for this species, which is not surprising given the poor signal-to-noise achieved experimentally [26]. We estimate that ca. 20% enrichment in $^{33}S$ would be ideal for measurement of the larger $^{33}S$ coupling, and the smaller value could probably be resolved from computer simulation and line-fitting of the spectra.

## 4. Conclusions and work in progress

The application of DFT methods has greatly increased the experimentalist's ability to correctly assign the EPR spectra of structurally uncertain free radicals; concomitantly the calculations allow structures to be determined by means of their agreement with EPR spectral data for species which are not sufficiently stable to isolate and characterize by diffraction methods. This powerful approach is now being applied to the intriguing field of binary sulfur–nitrogen radicals. In this paper, we have confirmed the validity of our approach by the excellent agreement between the calculated and experimental hfc constants of the well-characterized $[S_3N_2]^{+\bullet}$ radical. We can confidently assign the structure of $[S_4N_4]^{-\bullet}$ to the $C_{2v}$ partly opened cage species shown in Fig. 11. The cage molecule $[S_4N_5]^{-2\bullet}$ has a very similar geometry and electronic structure to that of its uncapped analogue $[S_4N_4]^{-\bullet}$ and consequently has very similar hfc constant values to the four equivalent N nuclei, which supports the calculated structure for $[S_4N_4]^{-\bullet}$.

Our calculations suggest that many hitherto under-investigated S,N ring and cage radicals (i.e. $[S_3N_3]^{\bullet}$, $[S_4N_2]^{+\bullet}$, $[S_4N_2]^{-\bullet}$, $[S_4N_3]^{\bullet}$ and $[S_4N_5]^{\bullet}$) may be detectable in solution under favorable conditions, or by incorporation into host lattices of related diamagnetic salts or compounds. They also suggest that $^{33}S$ hfc data will be of great assistance in the definitive assignment of several controversial EPR spectra measured for as yet unconfirmed S,N radicals such as $[SNS]^{\bullet}$ and $[NSN]^{-\bullet}$. It is recognized, however, that the synthesis of $^{33}S$-labeled precursors will be both synthetically challenging and expensive.

## Acknowledgements

This work was supported by the NSERC-Canada in the form of Discovery Grant awards to R.T.B. and T.C. and by the Academy of Finland (H.M.T.). T.L.R. acknowledges the NSERC for a PGS-D scholarship and the Alberta Ingenuity Fund for a Doctoral Scholar award. The University of Lethbridge Travel Fund and the Faculty of Arts and Science helped to defray the costs of the delivery of the oral form of this paper. R.T.B. thanks Dr. J.-P. Majoral of LCC-Toulouse, France for hospitality on a Sabbatical leave where this paper was written. We thank the referees for helpful comments.

## Appendix A. Supplementary material

Supplementary data associated with this article can be found, in the online version, at doi:10.1016/j.jorganchem.2006.11.026.

## References

[1] (a) T. Chivers, A Guide to Chalcogen-Nitrogen Chemistry, World Scientific Publishing, Singapore, 2005;
(b) T. Chivers, Chem. Rev. 85 (1985) 341.
[2] (a) D. Chapman, A.G. Massey, Trans. Faraday Soc. 58 (1962) 1291;
(b) D.A.C. McNeil, M. Murray, M.C.R. Symons, J. Chem. Soc. A 7 (1967) 1019;
(c) S.A. Lipp, J.J. Chang, W.L. Jolly, Inorg. Chem. 9 (1970) 1970;
(d) S.A. Lipp, W.L. Jolly, Inorg. Chem. 10 (1971) 33;
(e) R.J. Gillespie, P.R. Ireland, J.E. Vekris, Can. J. Chem. 53 (1975) 3147;
(f) J. Giordan, H. Bock, M. Eiser, H.W. Roesky, Phosphorus, Sulfur, Silicon Relat. Elem. 13 (1982) 19;
(g) K.F. Preston, J.P. Charland, L.H. Sutcliffe, Can. J. Chem. 66 (1988) 1299;
(h) E. Aware, J. Passmore, K.F. Preston, L.H. Sutcliffe, Can. J. Chem. 66 (1988) 1176;
(i) K.M. Johnson, K.F. Preston, L.H. Sutcliffe, Magn. Reson. Chem. 26 (1988) 1015;
(j) F. Mistry, F.G. Herring, A. Haas, F. Aubke, J. Fluorine Chem. 66 (1994) 147.
[3] (a) T. Chivers, I. Drummond, J. Chem. Soc., Chem. Commun. (1973) 734;
(b) T. Chivers, I. Drummond, Inorg. Chem. 13 (1974) 1222;
(c) T. Chivers, W.G. Laidlaw, R.T. Oakley, M. Trsic, J. Am. Chem. Soc. 102 (1980) 5773.
[4] G. Domschke, R. Mayer, S. Bleisch, A. Bartl, A. Staško, Magn. Reson. Chem. 28 (1990) 797.
[5] K.F. Preston, L.H. Sutcliffe, Magn. Reson. Chem. 28 (1990) 189.
[6] R.T. Oakley, Prog. Inorg. Chem. 36 (1988) 299.
[7] (a) J.M. Rawson, A. Alberola, A. Whalley, J. Mater. Chem. 16 (2006) 2560;
(b) M. Jennings, K.E. Preuss, J. Wu, Chem. Commun. (2006) 341;
(c) S.M. Mattar, Chem. Phys. Lett. 427 (2006) 438;
(d) A.A. Leitch, C.E. McKenzie, R.T. Oakley, R.W. Reed, J.F. Richardson, L.D. Sawyer, Chem. Commun. (2006) 1088;
(e) S.M. Mattar, J. Sanford, A.D. Goodfellow, Chem. Phys. Lett. 418 (2006) 30;
(f) H.F. Lau, V.W.L. Ng, L.L. Koh, G.K. Tan, L.Y. Goh, T.L. Roemmele, S.D. Seagrave, R.T. Boeré, Angew. Chem., Int. Ed. 45 (2006) 4498;
(g) C.Y. Ang, R.T. Boeré, L.Y. Goh, L.L. Koh, S.L. Juan, G.K. Tan, X. Yu, Chem. Commun. (2006) 4735;
(h) R.T. Oakley, R.W. Reed, C.M. Robertson, J.F. Richardson, Inorg. Chem. 44 (2005) 1837;
(i) S.S. Staniland, W. Fujita, U. Yoshikatsu, K. Awaga, P.J. Camp, S.J. Clark, N. Robertson, Inorg. Chem. 44 (2005) 546;
(j) A. Decken, A. Mailman, S.M. Mattar, J. Passmore, Chem. Commun. (2005) 2366;
(k) J.M. Rawson, J. Luzon, F. Palacio, Coord. Chem. Rev. 249 (2005) 2631;
(l) J. Luzon, J. Campo, F. Palacio, G.J. McIntyre, J.M. Rawson, Polyhedron 24 (2005) 2579;
(m) R.T. Boeré, T.L. Roemmele, Phosphorous, Sulfur Silicon Relat. Elem. 179 (2004) 875;
(n) K.V. Shuvaev, V.A. Bagryansky, N.P. Gritsan, A.Y. Makarov, Y.N. Molin, A.V. Zibarev, Mendeleev Commun. (2003) 178;
(o) P. Kaszynski, J. Phys. Chem. A 105 (2001) 7615;
(p) J.M. Farrar, M.K. Patel, P. Kaszynski, V.G. Young Jr., J. Org. Chem. 65 (2000) 931;
(q) V. Chandrasekhar, T. Chivers, M. Parvez, I. Vargas-Baca, T. Ziegler, Inorg. Chem. 36 (1997) 4772.
[8] R.T. Boeré, T.L. Roemmele, Coord. Chem. Rev. 210 (2000) 369.
[9] (a) L. Hermosilla, P. Calle, J.M. García de la Vega, C. Siero, J. Phys. Chem. A 109 (2005) 1114;
(b) L. Hermosilla, P. Calle, J.M. García de la Vega, C. Siero, J. Phys. Chem. A 109 (2005) 7626.
[10] J. Gassmann, J. Fabian, Magn. Reson. Chem. 34 (1996) 913.
[11] (a) A. Armstrong, T. Chivers, H.M. Tuononen, Inorg. Chem. 44 (2005) 5778;
(b) T. Chivers, D.J. Eisler, J.S. Ritch, H.M. Tuononen, Angew. Chem., Int. Ed. 44 (2005) 4953;

(c) T. Chivers, D.J. Eisler, C. Fedorchuk, C. Schatte, H.M. Tuononen, R.T. Boeré, Chem. Commun. 31 (2005) 3930;
(d) A.F. Armstrong, T. Chivers, H.M. Tuononen, M. Parvez, R.T. Boeré, Inorg. Chem. 44 (2005) 7981;
(e) H.M. Tuononen, A.F. Armstrong, Inorg. Chem. 44 (2005) 8277;
(f) T. Chivers, D.J. Eisler, C. Fedorchuk, C. Schatte, H.M. Tuononen, R.T. Boeré, Inorg. Chem. 45 (2006) 2119;
(g) H.M. Tuononen, A.F. Armstrong, Dalton Trans. (2006) 1885.
[12] M.J. Frisch et al., GAUSSIAN-98 (Revision A11), Gaussian, Inc., Wallingford, CT, 1998.
[13] H. Partridge, J. Chem. Phys. 90 (1989) 1043.
[14] (a) H.-T. Chen, J.-J. Ho, J. Phys. Chem. A 109 (2005) 2564;
(b) W.A. Pryor, K.N. Houk, C.S. Foote, J.M. Fukuto, L.J. Ignarro, G.L. Squadrito, K.J.A. Davies, Am. J. Physiol.-Regul. Integr. Comp. Physiol. 291 (2006) R491;
(c) P.P. Dendy, P. Wardman, Brit. J. Radiol. 79 (2006) 545;
(d) T. Colman-Saizarbitoria, P. Boutros, A. Amesty, A. Bahsas, Y. Mathison, M.D. Garrido, A. Israel, J. Ethnopharmacol. 106 (2006) 327;
(e) W. Macyk, A.A. Franke, G.Y. Stochel, Coord. Chem. Rev. 249 (2005) 2437;
(f) K.M. Miranda, L. Ridnour, M. Esprey, D. Citrin, D. Thomas, D. Mancardi, S. Donzelli, D.A. Wink, T. Katori, C.G. Tocchetti, M. Ferlito, N. Padocci, J.M. Fukuto, Prog. Inorg. Chem. 54 (2005) 349.
[15] K.P. Huber, G. HerzbergConstants of Diatomic Molecules, vol. IV, Van Nostrand Reinhold, New York, 1979.
[16] J. Czernak, O. Zivny, Chem. Phys. 303 (2004) 137.
[17] CSD Version 5.27 (November 2005) searched by ConQuest Version 1.8, Cambridge Crystallographic Data Centre, Cambridge, UK, ©, 2006.
[18] M.B. Hursthouse, M. Motevalli, J. Chem. Soc., Dalton Trans. (1979) 1362.
[19] B. Vollmer, S. Wocadlo, W. Massa, K. Dehnicke, Z. Anorg. Allg. Chem. 622 (1996) 1306.
[20] J.M. Dyke, A. Morris, I.R. Trickle, J. Chem. Soc., Faraday Trans. 73 (1977) 147.
[21] (a) A. Carrington, D.H. Levy, J. Chem. Phys. 44 (1966) 1298;
(b) A. Carrington, B.J. Howard, D.H. Levy, J.C. Robertson, Mol. Phys. 15 (1968) 187;
(c) H. Uehara, Y. Morino, Mol. Phys. 17 (1969) 239;
(d) E. Hirota, J. Phys. Chem. 87 (1983) 3375;
(e) J.R. Anacona, P.B. Davies, Chem. Phys. Lett. 108 (1984) 128;
(f) J.R. Anacona, P.B. Davies, Infrared Phys. 25 (1985) 233.
[22] (a) A. Carrington, B.J. Howard, D.H. Levy, J.C. Robertson, Mol. Phys. 15 (1968) 187;
(b) T. Amano, S. Saito, E. Hirota, Y. Morino, J. Mol. Spectrosc. 32 (1969) 97;
(c) S.K. Lee, H. Ozeki, S. Saito, Astrophys. J. Suppl. S 98 (1995) 351.
[23] See for example: R.J. Miller, D. Feller, J. Phys. Chem. 98 (1994) 10375.
[24] Although the theoretical calculations give a state which is energetically an average of the two $J = 1/2$ and $J = 3/2$ states, these states share the same electron and spin densities. Hence, the calculated Fermi contact interaction is the same for both values of $J$.
[25] H.P. Fritz, R. Bruchhaus, Z. Anorg. Allg. Chem. 525 (1985) 214.
[26] H.P. Fritz, R. Bruchhaus, Electrochim. Acta 29 (1984) 947.
[27] J. Bojes, P.M. Boorman, T. Chivers, Inorg. Nucl. Chem. Lett. 12 (1976) 551.
[28] (a) R. Faggiani, R.J. Gillespie, C.J.L. Lock, J.D. Tyrer, Inorg. Chem. 17 (1978) 2975;
(b) U. Thewalt, K. Berhalter, P. Miller, Acta Crystallogr. 838 (1982) 1280;
(c) J.P. Johnson, J. Passmore, P.S. White, A.J. Banister, A.G. Kendrick, Acta Crystallogr., Sect. C 43 (1987) 1651;
(d) T.S. Cameron, A. Mailman, J. Passmore, K.V. Shuvaev, Inorg. Chem. 44 (2005) 6524.
[29] M.T. Nguyen, R. Flamming, N. Goldberg, H. Schwarz, Chem. Phys. Lett. 236 (1995) 201.
[30] (a) R.D. Brown, P.S. Elmes, D. McNaughton, J. Mol. Spectrosc. 140 (1990) 390;
(b) P. Hassanzadeh, L. Andrews, J. Am. Chem. Soc. 114 (1992) 83.
[31] (a) Y. Yamaguchi, Y. Xie, R.S. Grev, H.F. Schaeffer III, J. Chem. Phys. 92 (1990) 3683;
(b) Y. Yamaguchi, Y. Xie, I.L. Alberts, R.S. Grev, H.F. Schaeffer III, J. Chem. Phys. 93 (1990) 5053;
(c) Y. Yamaguchi, I.L. Alberts, Y. Xie, H.F. Schaeffer III, J. Chem. Phys. 94 (1991) 1277;
(d) U. Kaldor, F. Sackler, Chem. Phys. Lett. 185 (1991) 185;
(e) A.B. Sannigrahi, S.D. Peyerimhoff, Int. J. Quantum Chem. 41 (1992) 413;
(f) R.C. Mawhinney, J.D. Goddard, Inorg. Chem. 42 (2003) 6323.
[32] S. Parsons, J. Passmore, Acc. Chem. Res. 27 (1994) 101.
[33] T. Borrmann, E. Lork, R. Mews, M.M. Shakirov, A.V. Zibarev, Eur. J. Inorg. Chem. (2004) 2452.
[34] (a) N. Burford, T. Chivers, R.T. Oakley, T. Oswald, Can. J. Chem. 62 (1984) 712;
(b) R.T. Boeré, R.T. Oakley, M. Shevalier, J. Chem. Soc., Chem. Commun. (1987) 110;
(c) C. Wentrup, P. Kambouris, Chem. Rev. 91 (1991) 363;
(d) N. Burford, T. Chivers, A.W. Cordes, W.G. Laidlaw, M.C. Noble, R.T. Oakley, P.N. Swepston, J. Am. Chem. Soc. 104 (1982) 1282.
[35] R. Appel, I. Ruppert, R. Milker, V. Bastian, Chem. Ber. 107 (1974) 380.
[36] R.T. Boeré, C.L. French, R.T. Oakley, A.W. Cordes, J.A. James, S.L. Craig, J.B. Graham, J. Am. Chem. Soc. 107 (1985) 7710.
[37] M. Herberhold, W. Ehrenreich, Angew. Chem. 94 (1982) 637; Angew. Chem., Int. Ed. Engl. 21 (1982) 633; Angew. Chem. Suppl. (1982) 1346.
[38] M. Herberhold, W. Ehrenreich, W. Buehlmeyer, K. Guldner, Chem. Ber. 119 (1986) 1424.
[39] T. Chivers, M. Hojo, Inorg. Chem. 23 (1984) 1526.
[40] C.M. Mikulski, P.J. Russo, M.S. Saran, A.G. Macdiarmid, A.F. Garito, A.J.A. Heeger, J. Am. Chem. Soc. 97 (1975) 6358.
[41] H.M. Tuononen, R. Suontamo, J. Valkonen, R.S. Laitinen, J. Phys. Chem. A 108 (2004) 5670, and references therein.
[42] (a) A. Bali, K.C. Malhotra, Aust. J. Chem. 29 (1976) 1111;
(b) E. Besenjei, G.K. Eigendorf, D.C. Frost, Inorg. Chem. 25 (1986) 4404.
[43] A.J. Banister, Z.V. Hauptman, A.G. Kendrick, R.W.H. Small, J. Chem. Soc., Dalton Trans. (1987) 915.
[44] S. Millefiori, A. Millefiori, C. D'Arrigo, Inorg. Chim. Acta 50 (1981) 167.
[45] K. Bestari, R.T. Oakley, A.W. Cordes, Can. J. Chem. 69 (1991) 94.
[46] (a) J. Bojes, T. Chivers, W.G. Laidlaw, M. Trsic, J. Am. Chem. Soc. 101 (1979) 4517;
(b) R. Jones, P.F. Kelly, D.J. Williams, J.D. Woollins, Polyhedron 6 (1987) 154;
(c) P.N. Jagg, P.F. Kelly, H.S. Rzepa, D.J. Williams, J.D. Woollins, W. Wylie, Chem. Commun. (1991) 942;
(d) A.J. Banister, M.I. Hansford, Z.V. Hauptman, A.W. Luke, S.T. Wait, W. Clegg, K.A. Jorgensen, J. Chem. Soc., Dalton Trans. (1990) 2793.
[47] (a) S.A. Fairhurst, K.F. Preston, L.H. Sutcliffe, Can. J. Chem. 62 (1984) 1124;
(b) S.A. Fairhurst, A. Hulme-Lowe, K.M. Johnson, L.H. Sutcliffe, J. Passmore, M.J. Schriver, Magn. Reson. Chem. 23 (1985) 828;
(c) S.A. Fairhurst, K.M. Johnson, L.H. Sutcliffe, K.F. Preston, A.J. Banister, Z.V. Hauptman, J. Passmore, J. Chem. Soc., Dalton Trans. (1986) 1986.
[48] (a) R.D. Smith, J. Chem. Soc., Dalton Trans. (1974) 478;
(b) T. Chivers, M.N.S. Rao, Can. J. Chem. 61 (1983) 1957;
(c) T. Chivers, A.W. Cordes, R.T. Oakley, W.T. Pennington, Inorg. Chem. 22 (1983) 2429;
(d) J.K. Zhu, B.M. Gimarc, Inorg. Chem. 22 (1983) 1996.

[49] (a) W.M. Lau, N.P.C. Westwood, M.H. Palmer, J. Chem. Soc., Chem. Commun. (1985) 752;
(b) W.M. Lau, N.P.C. Westwood, M.H. Palmer, J. Am. Chem. Soc. 108 (1986) 3229.
[50] P. Love, G. Myer, H.I. Kao, M.M. Labes, W.R. Junker, C. Elbaum, Ann. N. Y. Acad. Sci. 313 (1978) 745.
[51] (a) J. Bojes, T. Chivers, W.G. Laidlow, M. Trsic, J. Am. Chem. Soc. 101 (1979) 4517;
(b) R. Jones, P.F. Kelly, D.J. Williams, J.D. Woollins, Polyhedron 6 (1987) 1541;
(c) A.J. Banister, M.I. Hansford, Z.V. Hauptman, A.W. Luke, S.T. Wait, W. Clegg, K.A. Jorgensen, J. Chem. Soc., Dalton Trans. (1990) 2793;
(d) P.N. Jagg, P.F. Kelly, H.S. Rzepa, D.J. Williams, J.D. Woollins, W. Wylie, Chem. Commun. (1991) 942.
[52] T. Chivers, P.W. Codding, W.G. Laidlaw, S.W. Liblong, R.T. Oakley, M. Trsic, J. Am. Chem. Soc. 105 (1983) 1186.
[53] T. Chivers, M. Hojo, Inorg. Chem. 23 (1984) 2738.
[54] F. De Proft, P.W. Fowler, R.W.A. Havenith, P. von Ragué Schleyer, G. Van Lier, P. Geerlings, Chem. Eur. J. 10 (2004) 940.
[55] A.W. Cordes, R.F. Kruk, E.K. Gordon, Inorg. Chem. 4 (1965) 681.
[56] J.-R. Galan-Mascaros, A.M.Z. Slawin, J.D. Woollins, D.J. Williams, Polyhedron 15 (1996) 4603.
[57] I. Nevitt, H.S. Rzepa, J.D. Woollins, Spectrochim. Acta A 45 (1989) 367.
[58] P. Machmer, P.A.C. McNeil, M.C.R. Symons, Trans. Faraday Soc. 66 (1970) 1309.
[59] (a) T. Chivers, D.D. McIntyre, K.J. Schmidt, H.J. Vogel, J. Chem. Soc., Chem. Commun. (1990) 1341;
(b) T. Chivers, K.J. Schmidt, Can. J. Chem. 70 (1992) 710.
[60] R.J. Gillespie, J.P. Kent, J.F. Sawyer, D.R. Slim, J.D. Tyrer, Inorg. Chem. 20 (1981) 3799.
[61] (a) U. Müller, E. Conradi, U. Demant, K. Dehnicke, Angew. Chem., Int. Ed. 23 (1984) 237;
(b) A.W. Cordes, C.G. Marcellus, M.C. Noble, R.T. Oakley, W.T. Pennington, J. Am. Chem. Soc. 105 (1983) 6008.
[62] (a) M. Parvez, R.T. Boeré, S. Derrick, K.H. Moock, Acta Crystallogr., Sect. C 51 (1995) 2116;
(b) I. Ernest, W. Holick, G. Rihs, D. Schomburg, G. Shoham, D. Wenkert, R.B. Woodward, J. Am. Chem. Soc. 103 (1981) 1540;
(c) R.T. Boeré, K.H. Moock, S. Derrick, W. Hoogerdijk, K. Preuss, J. Yip, M. Parvez, Can. J. Chem. 71 (1993) 473.
[63] H. Chandra, D.N.R. Rao, M.C.R. Symons, J. Chem. Soc., Dalton Trans. (1987) 729.
[64] (a) R.A. Meinzer, D.W. Pratt, R.J. Myers, J. Am. Chem. Soc. 91 (1969) 6623;
(b) J.D. Williford, R.E. Van Reet, M.P. Eastman, K.B. Prater, J. Electrochem. Soc. 120 (1973) 1498.
[65] (a) M.J. Almond, G.A. Forsyth, D.A. Rice, A.J. Downs, T.L. Jeffery, K. Hagen, Polyhedron 8 (1989) 2631;
(b) W. Scherer, M. Spiegler, B. Pedersen, M. Tafipolsky, W. Hieringer, B. Reinhard, A.J. Downs, G.S. McGrady, Chem. Commun. (2000) 635.
[66] (a) T. Chivers, L. Fielding, W.G. Laidlaw, M. Trsic, Inorg. Chem. 18 (1979) 3379;
(b) W. Isenberg, R. Mews, Z. Naturforsch. B 37 (1982) 1388;
(c) J. Eicheer, P. Klingelhofer, U. Müller, K. Dehnicke, Z. Anorg. Allg. Chem. 514 (1984) 79.
[67] (a) C. Knapp, E. Lork, T. Borrmann, W.-D. Stohrer, R. Mews, Z. Anorg. Allg. Chem. 631 (2005) 1885;
(b) W. Isenberg, R. Mews, G.M. Sheldrick, R. Bartetzko, R. Gleiter, Z. Naturforsch. B 38 (1983) 1563.
[68] W. Flues, O.J. Scherer, J. Weiss, G. Wolmershäuser, Angew. Chem., Int. Ed. 15 (1976) 379.